Acta Cryst. (1973). A**29**, 585

The Short-Range Structure of Ti and Zr B.C.C. Solid Solutions containing the ω Phase. I. General Diffraction Theory and Development of Computational Techniques*

BY BERNARD BORIE,† STEPHEN L. SASS AND ALF ANDREASSEN‡

Department of Materials Science and Engineering, Cornell University, Ithaca, New York 14850, *U.S.A.*

(*Received* 14 *December* 1972; *accepted* 11 *April* 1973)

Certain Ti and Zr solid solutions containing the ω phase exhibit intensity distributions in reciprocal space which are partly diffuse. In an effort to understand the structural meaning of these diffraction patterns, we have developed new methods for the evaluation of the kinematic intensity sum for certain kinds of atomic arrangements which are not quite periodic. The methods are illustrated by their application to a simple model for these alloy systems. The model successfully reproduces some but not all of the features of observed intensity distributions.

Introduction

Alloys based on Ti or Zr containing elements such as V or Nb exhibit a b.c.c. solid solution (called the β phase) at high temperatures which can partially decompose upon cooling to a metastable structure called the ω phase. Silcock, Davies & Hardy (1955) and Bagaryatskii, Nosova & Tagunova (1955) have shown that the ω phase has a structure based on that of the β phase. If the primitive rhombohedral cell of the b.c.c. structure is indexed hexagonally, the resultant triply primitive cell has $c/a=(\frac{3}{8})^{1/2}$ with atomic positions $0,0,0$; $\frac{2}{3},\frac{1}{3},\frac{1}{3}$; $\frac{1}{3},\frac{2}{3},\frac{2}{3}$. Unless

$$-h+k+1=3q \qquad (1)$$

where q is an integer and the indices refer to the hexagonal cell, the structure factor F_{hkl} vanishes.

The hexagonal cell dimensions of the as-quenched ω phase have not been observed to differ from those of the parent structure; however the atomic positions become $0,0,0$; $\frac{2}{3},\frac{1}{3},\frac{1}{3}+u$; $\frac{1}{3},\frac{2}{3},\frac{2}{3}-u$. Extinction rule (1) is relaxed and after transformation extra Bragg maxima are observed in the diffraction pattern. Because each of the four cubic cell diagonals is equally likely to have been chosen for the hexagonal c axis, the diffraction pattern consists of the superposition of the patterns of the four variants of the system. For dilute alloys it is generally observed that $u=\frac{1}{6}$, though with increasing solute content the parameter u may be somewhat less (Sass & Borie, 1972).

In general, as exhibited by their diffraction patterns, there are also significant and systematic deviations from periodicity in more concentrated alloys. The most conspicuous features of the patterns are:

1. Those Bragg maxima common both to ω and β [that is, those compatible with extinction rule (1), here called fundamental reflections] are sharp. Those associated with the ω phase only (here called superstructure reflections) become diffuse.

2. The superstructure reflections are broadened mainly in directions perpendicular to **c***, resulting in planes of diffuse scattering of more or less constant l.

3. There is no diffuse scattering in the $hk0$ plane of reciprocal space.

4. The superstructure reflections are displaced from their normal positions in reciprocal space parallel to **c*** in a systematic way (for example, 001 and 002 are shifted toward each other).

5. The fundamental reflections decrease rapidly in intensity with distance from the origin in reciprocal space. This large apparent Debye–Waller factor is not of thermal origin.

These properties of the intensity distribution have recently been discussed at length by Sass (1972), particularly with regard to the systems Zr–Nb, Ti–V, and Ti–Nb. That none of them are related primarily to thermal motion is an observation derived from the neutron scattering experiments with an alloy of Zr–20 wt. % Nb of Keating, Axe & Moss (1973).

It is our purpose here to attempt to understand the structural meaning of these features of the diffraction patterns from alloy systems that can form the ω phase. We seek a model specifying atomic positions in the alloy for which the kinematic intensity sum may be evaluated, which will reproduce quantitatively the observed intensity distribution.

New techniques for finding the intensity for a non-periodic array of atoms are developed and in Part I applied to a first simple model for the atomic configuration. A result is obtained which with the aid of a computer gives the diffuse intensity distribution in reciprocal space. Certain features of our result are not in agreement with experiment. In Part II the diffraction theory

* Research sponsored by the U. S. Atomic Energy Commission under contract with the Union Carbide Corporation, the Metallurgy Branch of the U. S. Office of Naval Research, and the U. S. Air Force.

† Also at The Metals and Ceramics Division, Oak Ridge National Laboratory, Oak Ridge, Tennessee 37830, U.S.A.

‡ Present address: The Applied Physics Laboratory of Johns Hopkins University, Howard County Facility, 8623 Georgia Avenue, Silver Spring, Maryland 20910, U.S.A.

is applied to a model which reproduces in detail the observed intensity distribution.

Diffraction theory. I. Formulation of the problem

We assume that the four ω variants scatter independently, and hence intensities from them add. In what follows we confine our attention to only one variant.

We ask how, within one variant, can anomalous interference effects arise on transformation that could account for the observed intensity distribution. Fig. 1 illustrates how we have supposed that to happen. Before transformation the crystal consists of a set of hexagonal atomic planes in ABC stacking sequence. On transformation one plane moves up, its neighbor down (to form a graphite-like double layer), and its second neighbor doesn't move. With nuclei forming at random in the crystal there are clearly three equally likely ways that can happen: The unshifted plane may be A (subvariant ω_1), $B(\omega_2)$, or $C(\omega_3)$. The subvariants will scatter coherently, and there will therefore be interference effects not present in the pattern from a large periodic ω crystal.

Before transformation the position of any atom may be written $r_m = m_1\mathbf{a}_1 + m_2\mathbf{a}_2 + 2m_3\mathbf{a}_3 + \delta_{m3}$ where m_1, m_2, and m_3 are integers. Here $\mathbf{a}_1$ and $\mathbf{a}_2$ are the basis vectors of the hexagonal net. For reasons shortly to be apparent, we have taken $a_3 = c/6$, where c is the hexagonal lattice constant of the cell and is therefore three times the spacing of the hexagonal planes. Hence in terms of a_3, the spacing of the planes is $2a_3$. The A, B, or C character of a plane is specified by δ_{m3}. If the plane is A, $\delta_{m3} = 0$; if B, $\delta_{m3} = 2\mathbf{a}_1/3 + \mathbf{a}_2/3$; if C, $\delta_{m3} = \mathbf{a}_1/3 + 2\mathbf{a}_2/3$.

With $\mathbf{k} = 2\pi(h_1\mathbf{b}_1 + h_2\mathbf{b}_2 + h_3\mathbf{b}_3)$, the b_n's being reciprocal to the $\mathbf{a}_n$'s, we have for the kinematic intensity sum

$$I_\beta(\mathbf{k}) = \sum_m \sum_{m'} \exp[i\mathbf{k} \cdot (\mathbf{r}_m - \mathbf{r}_{m'})]$$
$$= \sum_{m_1}\sum_{m_2}\sum_{m_3}\sum_{m_1'}\sum_{m_2'}\sum_{m_3'} \exp[2\pi i\{(m_1 - m_1')h_1 + (m_2 - m_2')h_2 + 2(m_3 - m_3')h_3\} + i\mathbf{k} \cdot \delta_{m3} - \delta_{m3'})] . \quad (2)$$

Here we have taken the scattering factors, or neutron scattering lengths, for all atoms to be unity. For the system Zr–Nb with which we will ultimately be concerned, this is justifiable aside from a scaling factor since they are nearly identical for the two kinds of atoms for X-rays, electrons, and neutrons.

Alternatively, with $n_1 = m_1 - m_1'$, $n_2 = m_2 - m_2'$, $n_3 = m_3 - m_3'$, $\delta_{n3} = \delta_{m3} - \delta_{m3'}$, and N_n the total number of $n_1n_2n_3$ atomic pairs we can form in the crystal,

$$I_\beta(\mathbf{k}) = \sum_{n_1}\sum_{n_2}\sum_{n_3} N_n \times \exp[2\pi i(n_1h_1 + n_2h_2 + 2n_3h_3)]\langle \exp[i\mathbf{k} \cdot \delta_{n3}]\rangle . \quad (3)$$

The indicated average is necessary since in general δ_{n3} may depend on whether m_3' is A, B, or C. If n_3 is a multiple of three, $\delta_{m3} = \delta_{m3'}$, $\delta_{n3} = 0$, and

$$\langle \exp[i\mathbf{k} \cdot \delta_{n3}]\rangle = 1 . \quad (4)$$

But if $n_3 = 3q + 1$, and if the m_3'th plane is A, then the m_3th plane is B and $\mathbf{k} \cdot \delta_{n3} = \frac{2}{3}\pi(2h_1 + h_2)$. If the m_3'th plane is B, $\mathbf{k} \cdot \delta_{n3} = \mathbf{k} \cdot (\mathbf{a}_1/3 + 2\mathbf{a}_2/3 - 2\mathbf{a}_1/3 - \mathbf{a}_2/3) = \frac{2}{3}\pi(-h_1 + h_2)$.

Similarly for a C plane at m_3', $\mathbf{k} \cdot \delta_{n3} = \frac{2}{3}\pi(-h_1 - 2h_2)$. There results

$$\langle \exp[i\mathbf{k} \cdot \delta_{n3}]\rangle = \tfrac{1}{3}\{\exp[\tfrac{2}{3}\pi i(2h_1 + h_2)] + \exp[\tfrac{2}{3}\pi i(-h_1 + h_2)] + \exp[\tfrac{2}{3}\pi i(-h_1 - 2h_2]\} . \quad (5)$$

With $n_3 = 3q + 2$, we find that

$$\langle \exp[i\mathbf{k} \cdot \delta_{n3}]\rangle = \tfrac{1}{3}\{\exp[\tfrac{2}{3}\pi i(-2h_1 - h_2)] + \exp[\tfrac{2}{3}\pi i(h_1 - h_2)] + \exp[\tfrac{2}{3}\pi i(h_1 + 2h_2)]\} . \quad (6)$$

We now imagine that atomic displacements related to the formation of ω and illustrated schematically for the three subvariants by Fig. 1 occur. Note that the displacements must be parallel to $\mathbf{c}$ and therefore do not affect the A, B, or C character of a plane. If the final coordinate of a displaced atom in an ω cell is one-half, the displacement must have been $c/2 - c/3 = a_3$; or $c/2 - 2c/3 = -a_3$. Let κ_n be plus one if the $n_1n_2n_3$th atom is displaced $+a_3$; minus one if its displacement is $-a_3$; and zero if its position is unchanged after transformation. Define κ_0 similarly relative to the origin atom. Then the additional phase factor entering the

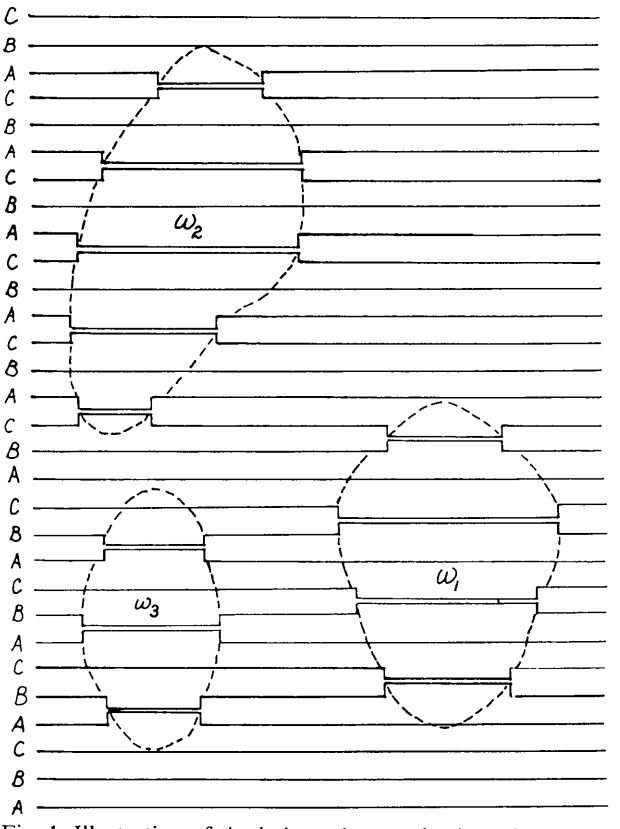

Fig. 1. Illustration of the independent nucleation of the three ω subvariants within a single variant.

kinematic sum after transformation is $\exp[2\pi i(\kappa_n-\kappa_0)h_3]$. But for different atomic pairs characterized by the same $n_1n_2n_3$, $\kappa_n-\kappa_0$ may be any integer between plus two and minus two. Hence after transformation equation (3) becomes

$$I(\mathbf{k})=\sum_{n_1}\sum_{n_2}\sum_{n_3}{}'N_n\exp[2\pi i(n_1h_1+n_2h_2+2n_3h_3)] \times\langle\exp[i\mathbf{k}\,.\,\boldsymbol{\delta}_{n3}]\rangle\langle\exp[2\pi i(\kappa_n-\kappa_0)h_3]\rangle\,, \quad (7)$$

the second indicated average being performed over all atomic pairs described by a common $n_1n_2n_3$. Performing the summation indicated by (7) is dependent on finding $\langle\exp[2\pi i(\kappa_n-\kappa_0)h_3]\rangle$.

Diffraction theory. II. Calculation of the intensity from a model

We evaluate equation (7) for a specific model of a partially transformed alloy. For simplicity we take the crystal to be composed of four equally likely regions: ω_1, ω_2, ω_3, and untransformed β. We assume that in each of the ω regions only integral cells exist; no ω cell fragments are allowed. We choose at random a hexagonal net plane to contain the origin, and we compute $\langle\exp[2\pi i(\kappa_n-\kappa_0)h_3]\rangle$ for all atomic pairs, one element of which is contained in the origin plane and the other in the n_3th hexagonal plane above it. At this point the A, B, or C character of a plane is arbitrary; we establish a labeling convention by calling the plane of the origin A. We specify criteria for deciding which of the four regions any given atom in the origin plane is in. If the atom is itself undisplaced ($\kappa_0=0$) and its neighbor in the preceding hexagonal net plane (at $x,y=\frac{1}{3},\frac{2}{3}$) is also undisplaced, the region is identified as untransformed. If its neighbor is displaced downward $c/6$, the region is ω_1. No upward displacement of the preceding neighbor of our undisplaced origin atom is allowed, since that would create a defective ω cell. If the origin atom is displaced downward $c/6$ ($\kappa_0=-1$), the region is ω_2. It must be followed by an undisplaced atom, and preceded by one displaced upward by $c/6$, as illustrated in Fig. 1. If the origin atom is displaced upward $c/6$ ($\kappa_0=+1$), the region is ω_3. These criteria for establishing the identy of the region containing the origin are illustrated schematically in Fig. 2.

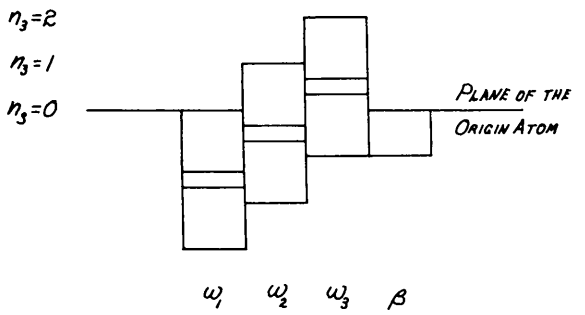

Fig. 2. Schematic representation of the atomic plane positions in the three subvariants and untransformed β.

Having specified the character of the immediate vicinity of the origin, we proceed to translate $n_1a_1+n_2a_2$ within the hexagonal net plane. As we do we will cross boundaries between the four equally likely regions. Table 1 gives the probability that we find ourselves in any of the four regions after having begun in a specified region (say region I), and after having crossed a specified number of boundaries. The Table is based on the assumption that any region has with equal probability neighboring regions of the other three kinds. Note that as the number of boundaries crossed increases the probabilities P_p (that after having crossed p boundaries one is in the same type region as that of the origin) and P'_p (that one is in a region different from that of the origin) approach their random value of one-quarter. It is shown in Appendix A that

$$P_p=\tfrac{1}{4}+\tfrac{3}{4}(-\tfrac{1}{3})^p \quad (8)$$

and

$$P'_p=\tfrac{1}{4}-\tfrac{1}{4}(-\tfrac{1}{3})^p\,. \quad (9)$$

Table 1. *Probabilities for translations in a plane composed of four distinctly different regions*

Number of boundaries crossed	Probability of terminating in region I	II	III	IV
0	1	0	0	0
1	0	$\frac{1}{3}$	$\frac{1}{3}$	$\frac{1}{3}$
2	$\frac{1}{3}$	$\frac{2}{9}$	$\frac{2}{9}$	$\frac{2}{9}$
3	$\frac{2}{9}$	$\frac{7}{27}$	$\frac{7}{27}$	$\frac{7}{27}$
4	$\frac{7}{27}$	$\frac{20}{81}$	$\frac{20}{81}$	$\frac{20}{81}$
p	P_p	P'_p	P'_p	P'_p

To describe the statistical character of the alloy for the component of translation parallel to **c**, we take a vertical column of material to be composed of two kinds of translational entities: integral ω cells of height c, and adjacent undisplaced planes (β regions) of height $c/3$. Clearly to pass from, say, subvariant ω_1 to ω_2 in such a column, we must traverse $(3q+1)$ β translational entities, since as is evident from Fig. 1 or 2 an ω_2 region is translated by $c/3$ relative to ω_1. Similarly, to pass from ω_1 to ω_3, there must be interposed $(3q+2)$ β translational entities.

Since by volume the alloy is one-quarter untransformed, and since a β entity is one-third the height of an ω cell, the two must exist in equal numbers in a vertical column. For simplicity we assume that the two entities are randomly distributed in the column; that is, the probability that an undisplaced atom begins an integral ω cell is one-half, and the probability that it is followed by another undisplaced atom, or that it begins a β entity, is one-half.

It is important to note that this simple model will not lead to the relatively large ω regions shown in Fig. 1, for which a certain amount of local order would be necessary. The Figure is also not intended to suggest the relative volumes of transformed and untransformed material used in this first model.

To compute $\langle\exp[2\pi i(\kappa_n-\kappa_0)h_3]\rangle$, we introduce a set of conditional probabilities σ_{n3}, the probability that

after having found an atom to be undisplaced in the origin plane, we traverse n_3 planes parallel to **c** and find n_3th atom also undisplaced. Note that as defined here, σ_{n_3} depends only on the two atoms being undisplaced; that is, that they terminate a translational entity, without regard to whether the entity is β or ω.

We may now write the contribution to $\langle \exp [2\pi i(\kappa_n - \kappa_0)h_3]\rangle$ for those atomic pairs which begin with the origin in, say, an ω_2 subvariant. The probability that the origin is in ω_2 is one-fourth; from Fig. 2, $\kappa_0 = -1$ so $\exp [-2\pi i\kappa_0 h_3] = \exp [2\pi i h_3]$. After having traversed p boundaries in the hexagonal net plane (at this point we describe the translation in the net plane in terms of the number of boundaries crossed; subsequently we will relate p to $n_1 + n_2$, the distance translated) the probability that we are still in an ω_2 region is P_p. In such a region, from Fig. 2, in a vertical column the atom at $n_3 = 1$ must be undisplaced. Hence σ_{n_3-1} is the probability that the n_3th atom in the column is undisplaced. The probability that the n_3th atom is displaced upward (and hence $\exp [2\pi i\kappa_n h_3] = \exp [2\pi i h_3]$) is σ_{n_3-2} [the probability that the (n_3-1)th atom is undisplaced] times one-half [the probability that it is followed by an integral ω cell, in which case the atom at $(n_3-1)+1$ must be displaced upward]. Similarly the probability that the n_3th atom is displaced downward is $\frac{1}{2}\sigma_{n_3-3}$. Hence the contribution to the average sought after beginning in ω_2, traversing p boundaries in the hexagonal plane and still finding ourselves in ω_2, and translating n_3 planes parallel to **c** is

$$\tfrac{1}{4} \exp [2\pi i h_3] P_p(\sigma_{n_3-1} + \tfrac{1}{2}\sigma_{n_3-2} \exp [2\pi i h_3] + \tfrac{1}{2}\sigma_{n_3-3} \exp [-2\pi i h_3]).$$

The probability that the hexagonal translation crossing p boundaries terminates in ω_3 is P'_p. Here from Fig. 2 the atom at $n_3 = 2$ is undisplaced. Hence the subscripts on σ_n must be reduced by one relative to the first case considered, and we have for the contribution to the average

$$\tfrac{1}{4} \exp [2\pi i h_3] P'_p(\sigma_{n_3-2} + \tfrac{1}{2}\sigma_{n_3-3} [2\pi i h_3] + \tfrac{1}{2}\sigma_{n_3-4} \exp [-2\pi i h_3]).$$

If the hexagonal translation terminates in either ω_1 or β (probability $2P'_p$), from Fig. 2 the atom at $n_3 = 0$ is undisplaced and the subscripts must be advanced by unity relative to the first case; the contribution is

$$\tfrac{1}{4} \exp [2\pi i h_3] 2P'_p(\sigma_{n_3} + \tfrac{1}{2}\sigma_{n_3-1} \exp [2\pi i h_3] + \tfrac{1}{2}\sigma_{n_3-2} \exp [-2\pi i h_3]).$$

Hence the total contribution to the average for those atomic pairs which begin with the origin in ω_2 is

$$\begin{aligned}\langle \exp [2\pi i(\kappa_n - \kappa_0)h_3]\rangle_2 &= \tfrac{1}{4} \exp [2\pi i h_3]\{P_p(\sigma_{n_3-1} \\ &+ \tfrac{1}{2}\sigma_{n_3-2} \exp [2\pi i h_3] + \tfrac{1}{2}\sigma_{n_3-3} \exp [-2\pi i h_3]) \\ &+ P'_p(\sigma_{n_3-2} + \tfrac{1}{2}\sigma_{n_3-3} \exp [2\pi i h_3] + \tfrac{1}{2}\sigma_{n_3-4} \\ &\times \exp [-2\pi i h_3]) + 2P'_p(\sigma_{n_3} + \tfrac{1}{2}\sigma_{n_3-1} \exp [2\pi i h_3] \\ &+ \tfrac{1}{2}\sigma_{n_3-2} \exp [-2\pi i h_3])\} . \qquad (10)\end{aligned}$$

After substitution of equations (8) and (9) for P_p and P'_p, and some rearrangement, equation (10) becomes

$$\begin{aligned}\langle \exp [2\pi i(\kappa_n - \kappa_0)h_3]\rangle_2 &= \tfrac{1}{16}[1 - (-\tfrac{1}{3})^p] \exp [2\pi i h_3] \\ &\times \{(2\sigma_{n_3} + \sigma_{n_3-1} + \sigma_{n_3-2}) + \exp [2\pi i h_3](\sigma_{n_3-1} \\ &+ \tfrac{1}{2}\sigma_{n_3-2} + \tfrac{1}{2}\sigma_{n_3-3}) + \exp [-2\pi i h_3](\sigma_{n_3-2} + \tfrac{1}{2}\sigma_{n_3-3} \\ &+ \tfrac{1}{2}\sigma_{n_3-4})\} + \tfrac{1}{4}(-\tfrac{1}{3})^p(\sigma_{n_3-1} \exp [2\pi i h_3] \\ &+ \tfrac{1}{2}\sigma_{n_3-2} \exp [4\pi i h_3] + \tfrac{1}{2}\sigma_{n_3-3}) . \qquad (11)\end{aligned}$$

There exists a relation among the σ_n's. Since σ_n is the probability that the nth plane is undisplaced, $\frac{1}{2}\sigma_{n-1}$ that it is displaced upward, and $\frac{1}{2}\sigma_{n-2}$ that it is displaced downward,

$$\sigma_n + \tfrac{1}{2}\sigma_{n-1} + \tfrac{1}{2}\sigma_{n-2} = 1 . \qquad (12)$$

Identity (12) must hold for all n. Hence (11) becomes

$$\begin{aligned}\langle \exp [2\pi i(\kappa_n - \kappa_0)h_3]\rangle_2 &= \tfrac{1}{4}[1 - (-\tfrac{1}{3})^p] \exp [2\pi i h_3] \\ &\times \{\tfrac{1}{2} + \tfrac{1}{4} \exp [2\pi i h_3] + \tfrac{1}{4} \exp [-2\pi i h_3]\} \\ &+ \tfrac{1}{4}(-\tfrac{1}{3})^p(\sigma_{n_3-1} \exp [2\pi i h_3] + \tfrac{1}{2}\sigma_{n_3-2} \exp [4\pi i h_3] \\ &+ \tfrac{1}{2}\sigma_{n_3-3}) .\end{aligned}$$

Or, with the notation

$$\mathscr{F} = \tfrac{1}{2} + \tfrac{1}{4} \exp [2\pi i h_3] + \tfrac{1}{4} \exp [-2\pi i h_3] \qquad (13)$$

we have that

$$\begin{aligned}\langle \exp [2\pi i(\kappa_n - \kappa_0)h_3]\rangle_2 &= \tfrac{1}{4}[1 - (-\tfrac{1}{3})^p] \exp [2\pi i h_3]\mathscr{F} \\ &+ \tfrac{1}{4}(-\tfrac{1}{3})^p(\sigma_{n_3-1} \exp [2\pi i h_3] + \tfrac{1}{2}\sigma_{n_3-2} \exp [4\pi i h_3] \\ &+ \tfrac{1}{2}\sigma_{n_3-3}) . \qquad (14)\end{aligned}$$

$\mathscr{F}$ is essentially the average structure factor per atom; that is, one-half of the atoms in a hexagonal plane are undisplaced (all of them in β regions and one-third of them in ω regions), one-quarter of them are displaced upward, and one-quarter of them downward.

By a similar development, we find that beginning with the origin in an ω_3 subvariant,

$$\begin{aligned}\langle \exp [2\pi i(\kappa_n - \kappa_0)h_3]\rangle_3 &= \tfrac{1}{4}[1 - (\tfrac{1}{3})^p] \exp [-2\pi i h_3]\mathscr{F} \\ &+ \tfrac{1}{4}(-\tfrac{1}{3})^p(\sigma_{n_3-2} \exp [-2\pi i h_3] + \tfrac{1}{2}\sigma_{n_3-3} \\ &+ \tfrac{1}{2}\sigma_{n_3-4} \exp [-4\pi i h_3]) . \qquad (15)\end{aligned}$$

The result for ω_1 and β regions is the same, and the two may be combined:

$$\begin{aligned}\langle \exp [2\pi i(\kappa_n - \kappa_0)h_3]\rangle_{1+\beta} &= \tfrac{1}{2}[1 - (-\tfrac{1}{3})^p]\mathscr{F} \\ &+ \tfrac{1}{2}(-\tfrac{1}{3})^p(\sigma_{n_3} + \tfrac{1}{2}\sigma_{n_3-1} \exp [2\pi i h_3] \\ &+ \tfrac{1}{2}\sigma_{n_3-2} \exp [-2\pi i h_3]) . \qquad (16)\end{aligned}$$

Equations (14), (15), and (16) may now be combined to yield the average sought:

$$\begin{aligned}\langle \exp [2\pi i(\kappa_n - \kappa_0)h_3]\rangle &= [1 - (-\tfrac{1}{3})^p]\mathscr{F}^2 \\ &+ (-\tfrac{1}{3})^p\{\tfrac{1}{2}\sigma_{n_3} + \tfrac{1}{4}\sigma_{n_3-3} + \tfrac{1}{2}\sigma_{n_3-1} \exp [2\pi i h_3] \\ &+ \tfrac{1}{2}\sigma_{n_3-2} \exp [-2\pi i h_3] + \tfrac{1}{8}\sigma_{n_3-2} \exp [4\pi i h_3] \\ &+ \tfrac{1}{8}\sigma_{n_3-4} \exp [-4\pi i h_3]\} . \qquad (17)\end{aligned}$$

Introduce the notation

$$\psi_{n3}=(\tfrac{1}{2}\sigma_{n3}+\tfrac{1}{4}\sigma_{n3-3}-\tfrac{3}{8})+(\tfrac{1}{2}\sigma_{n3-1}-\tfrac{1}{4})\exp[2\pi i h_3]+(\tfrac{1}{2}\sigma_{n3-2}-\tfrac{1}{4})\exp[-2\pi i h_3]+(\tfrac{1}{8}\sigma_{n3-4}-\tfrac{1}{16})\exp[4\pi i h_3]+(\tfrac{1}{8}\sigma_{n3-4}-\tfrac{1}{16})\exp[-4\pi i h_3]\,. \quad (18)$$

In the above expression $\mathscr{F}^2$ as given by equation (13) has been used. Then

$$\langle\exp[2\pi i(\kappa_n-\kappa_0)h_3]\rangle=\mathscr{F}^2+(-\tfrac{1}{3})^p\psi_{n3}\,. \quad (19)$$

Though we have derived equation (19) by beginning with the origin on an A plane, an identical result clearly obtains with the origin on B or C, since the A, B, or C character of a plane is contained in the factor $\langle\exp[i\mathbf{k}\,.\,\boldsymbol{\delta}_{n3}]\rangle$ of equation (7). Note from (18) that ψ_{n3} converges to zero for large n_3, since in that case σ_{n3} is simply the probability that an atom is undisplaced namely one-half. In Appendix B, two additional necessary properties of ψ_{n3} are displayed.

This result may now be substituted into equation (7). With equation (3) for I_β, we obtain

$$I(\mathbf{k})=\mathscr{F}^2I_\beta+\sum_{n_1}\sum_{n_2}\sum_{n_3}N_n\exp[2\pi i(n_1h_1+n_2h_2+2n_3h_3)]\langle\exp[i\mathbf{k}\,.\,\boldsymbol{\delta}_{n3}]\rangle\psi_{n3}\sum_{p=o}^{n_1+n_2}S_p^{n_1+n_2}(-\tfrac{1}{3})^p. \quad (20)$$

Here $S_p^{n_1+n_2}$ is the probability that in a translation of $n_1\mathbf{a}_1+n_2\mathbf{a}_2$, p boundaries are crossed. If each translation of $\mathbf{a}_1$ or $\mathbf{a}_2$ provides an opportunity for a fault, clearly p must be between zero and n_1+n_2. To evaluate the sum over p, let α be the probability that a boundary is crossed in a translation of $\mathbf{a}_1$ or $\mathbf{a}_2$. Assume that the distribution of boundaries is random. Then $S_0^{n_1+n_2}=(1-\alpha)^{n_1+n_2}$. For one boundary, we have $S_1^{n_1+n_2}=(n_1+n_2)(1-\alpha)^{n_1+n_2-1}\alpha$. The factor n_1+n_2 results from the fact that there are n_1+n_2 places to put the single boundary. For two boundaries, $S_2^{n_1+n_2}=\frac{1}{2}(n_1+n_2)(n_1+n_2-1)(1-\alpha)^{n_1+n_2-2}\alpha^2$. Here there are n_1+n_2 places for the first boundary and n_1+n_2-1 for the second one. We must divide by two since an interchange of the boundaries does not constitute a new configuration. In general

$$\sum_{p=0}^{n_1+n_2}S_p^{n_1+n_2}(-\tfrac{1}{3})^p=(1-\alpha)^{n_1+n_2}+(n_1+n_2)(1-\alpha)^{n_1+n_2-1}\times(-\tfrac{1}{3}\alpha)+\tfrac{1}{2}(n_1+n_2)(n_1+n_2-1)(1-\alpha)^{n_1+n_2-2}(-\tfrac{1}{3}\alpha)^2+\ldots+\frac{(n_1+n_2)!}{(n_1+n_2-p)!\,p!}(1-\alpha)^{n_1+n_2-p}(-\tfrac{1}{3}\alpha)^p+\ldots=[(1-\alpha)+(-\tfrac{1}{3}\alpha)]^{n_1+n_2}=\eta^{n_1+n_2} \quad (21)$$

where $\eta=1-4\alpha/3$. With this result equation (20) becomes

$$I(\mathbf{k})=\mathscr{F}^2I_\beta+N\sum_{n_1}(\eta\exp[2\pi ih_1])^{n_1}\sum_{n_2}(\eta\exp[2\pi ih_2])^{n_2}\times\sum_{n_3}\psi_{n3}\langle\exp[i\mathbf{k}\,.\,\boldsymbol{\delta}_{n3}]\rangle\exp[4\pi in_3h_3]\,. \quad (22)$$

The first term of equation (22) gives sharp Bragg maxima only at the fundamental positions in reciprocal space. They are 'fundamental reflections' in the sense that they depend only on the average structure. The factor $\mathscr{F}^2$ on I_β accounts for the experimentally observed static pseudo Debye–Waller factor on these reflections. Diffraction effects related to short-range fluctuations about the average structure are contained in the second term of (22). However, here we are concerned not with short-range order among chemically different atoms, but order among different structural configurations.

Because η is less than one and ψ_{n3} approaches zero for large n_3, the three sums of equation (22) all converge. We are thus justified in making the infinite-crystal approximation; that is, we may replace N_n by N, the total number of atoms in the crystal, and remove it from the triple sum as indicated in (22).

In what follows we will be concerned primarily with $I_D=I-\mathscr{F}^2I_\beta$, the diffuse part of the intensity distribution related to the local structural order. With the notation

$$G(h_1h_2)=\sum_{n_1}\sum_{n_2}(\eta\exp[2\pi ih_1])^{n_1}(\eta\exp[2\pi ih_2])^{n_2} \quad (23)$$

and

$$Q(h_1h_2h_3)=\sum_{n_3}\psi_{n3}\langle\exp[i\mathbf{k}\,.\,\boldsymbol{\delta}_{n3}]\rangle\exp[4\pi in_3h_3] \quad (24)$$

we have from equation (22) that

$$I_D/N=GQ\,. \quad (25)$$

The detailed evaluation of the two-dimensional diffuse function $G(h_1h_2)$ is described in Appendix C. We discuss here briefly some of its properties. Because it is essentially a two-dimensional Fourier series whose 00 Fourier coefficient is unity, we must have for any η that

$$\int_0^1\int_0^1G(h_1h_2)\mathrm{d}h_1\mathrm{d}h_2=1\,. \quad (26)$$

For large η (or small α) it consists of peaks centered on integral h_1 and h_2. The peaks broaden as η decreases. At $\eta=0$ (or $\alpha=\frac{3}{4}$), $G(h_1h_2)$ is structureless and equal to unity. That this is so results from the fact that $\alpha=\frac{3}{4}$ causes a random distribution of the four kinds of regions in the hexagonal net plane. In the plane the probability that an atom has a neighbor with a like environment is $1-\alpha=\frac{1}{4}$. The probability that its neighbor has any one of the other three possible environments is $\alpha/3=\frac{1}{4}$. There is thus no structural short-range order in the net plane.

Though it involves a sum only over n_3, Q depends on all three variables because $\mathbf{k}\,.\,\boldsymbol{\delta}_{n3}$ contains h_1 and h_2. Its evaluation derives from ψ_{n3} as given in terms of σ_{n3} by equation (18). Given that $\sigma_0=1$ and $\sigma_1=\frac{1}{2}$, equation (12) may be used as a recursion formula for the generation of subsequent σ_{n3}'s. This procedure, with the evaluation of ψ_{n3} from equation (18) and the summation of equation (24) to give $Q(h_1h_2h_3)$, may be

readily performed with a computer. Because (18) contains σ_{n3-4}, ψ_0, ψ_1, ψ_2, and ψ_3 must be treated as special cases.

We compute ψ_1. The contribution to $\langle \exp[2\pi i(\kappa_n - \kappa_0)h_3]\rangle$ for those pairs beginning in ω_2, for $n_3 = 1$, is

$$\langle \exp[2\pi i(\kappa_n-\kappa_0)h_3]\rangle_2 = \tfrac{1}{4}\exp[2\pi i h_3][\tfrac{1}{4}+\tfrac{3}{4}(-\tfrac{1}{3})^p](1) + \tfrac{1}{4}\exp[2\pi i h_3][\tfrac{1}{4}-\tfrac{1}{4}(-\tfrac{1}{3})^p] \times (1+\exp[2\pi i h_3]+\exp[-2\pi i h_3]) . \quad (27)$$

This expression follows from Fig. 2. In ω_2 the probability that the plane for $n_3 = 1$ is undisplaced is unity. In ω_1 or β the first plane may be undisplaced (probability one-half) or it may be displaced upward (probability one-half). In ω_3 it must be displaced downward. Hence $2(\frac{1}{2}+\frac{1}{2}\exp[2\pi i h_3])+\exp[-2\pi i h_3]$ must be the coefficient of $\frac{1}{4}\exp[2\pi i h_3]P'_p$. After simplification (27) reduces to

$$\langle \exp[2\pi i(\kappa_n-\kappa_0)h_3]\rangle_2 = \tfrac{1}{4}\exp[2\pi i h_3]\mathscr{F}[1-(-\tfrac{1}{3})^p] + (-\tfrac{1}{3})^p\tfrac{1}{4}\exp[2\pi i h_3] . \quad (28)$$

Similarly

$$\langle \exp[2\pi i(\kappa_n-\kappa_0)h_3]\rangle_3 = \tfrac{1}{4}\exp[-2\pi i h_3]\mathscr{F}[1-(-\tfrac{1}{3})^p] + (-\tfrac{1}{3})^p\tfrac{1}{4}\exp[-4\pi i h_3] \quad (29)$$

and

$$\langle \exp[2\pi i(\kappa_n-\kappa_0)h_3]\rangle_{1+\beta} = \tfrac{1}{2}\mathscr{F}[1-(-\tfrac{1}{3})^p] + (-\tfrac{1}{3})^p(\tfrac{1}{4}+\tfrac{1}{4}\exp[2\pi i h_3]) . \quad (30)$$

The combination of (28), (29), and (30) gives

$$\langle \exp[2\pi i(\kappa_n-\kappa_0)h_3]\rangle = \mathscr{F}^2 + (-\tfrac{1}{3})^p(\tfrac{1}{4}+\tfrac{1}{2}\exp[2\pi i h_3] + \tfrac{1}{4}\exp[-4\pi i h_3]-\mathscr{F}^2) . \quad (31)$$

Hence from (19), and with $\mathscr{F}^2$ from (13),

$$\psi_1 = -\tfrac{1}{8}+\tfrac{1}{4}\exp[2\pi i h_3]-\tfrac{1}{4}\exp[-2\pi i h_3] - \tfrac{1}{16}\exp[4\pi i h_3]+\tfrac{3}{16}\exp[-4\pi i h_3] . \quad (32)$$

Similar expressions for $n_3 = 0$, 2, and 3 are

$$\psi_0 = \tfrac{5}{8}-\tfrac{1}{4}\exp[2\pi i h_3]-\tfrac{1}{4}\exp[-2\pi i h_3] - \tfrac{1}{16}\exp[4\pi i h_3]-\tfrac{1}{16}\exp[-4\pi i h_3] \quad (33)$$

$$\psi_2 = -\tfrac{1}{4}+\tfrac{1}{4}\exp[-2\pi i h_3]+\tfrac{1}{16}\exp[4\pi i h_3] - \tfrac{1}{16}\exp[-4\pi i h_3] \quad (34)$$

$$\psi_3 = \tfrac{3}{16}-\tfrac{1}{8}\exp[2\pi i h_3]-\tfrac{1}{16}\exp[-4\pi i h_3] . \quad (35)$$

Yakel (1972) has pointed out that an alternative to the enumeration of ψ_n for $n<4$ is to use the recursion formula (12) to advance the subscripts on the σ_n's in expression (18) for ψ_n.

Result and discussion

Fig. 3 illustrates $Q(h_1 0 H_3)$ evaluated as described above. It is plotted in terms of $H_3 = 6h_3$ which is equal to the Miller index l at its integer values. The computer calculation of the summation of equation (24) was terminated at $|n_3| = 16$. The function is periodic in h_1 with repeat interval three, and in H_3 with repeat interval six. For $3 < H_3 < 6$, Q may be obtained from Fig. 3 and the fact that the point $h_1, H_3 = \frac{3}{2}, 3$ is an inversion center. The positions of the sharp fundamental Bragg maxima are indicated on the map by closed circles.

There are certain aspects of our calculation which suggest that it is an approach to physical reality. We have correctly separated the pattern into sharp fundamentals and superstructure reflections which are diffuse. The diffuse peaks tend to be broader in directions perpendicular to **c*** as observed, though this broadening is frequently observed to be more exaggerated than is shown in Fig. 3.

As has been pointed out, diffraction patterns of more concentrated alloys often indicate that the structural parameter u is less than $\frac{1}{6}$. For the part of the pattern represented by Fig. 3, smaller u causes the intensity of $hkl = 103$ to be much greater than 203, while they are shown to be the same in the figure.

Our calculation is easily modified to account for this. To cause F_{203} to vanish, u must be $\frac{1}{9}$. If we choose $a_3 = c/9$, equation (3) becomes

$$I_\beta(\mathbf{k}) = \sum_{n_1}\sum_{n_2}\sum_{n_3} N_n \exp[2\pi i(n_1h_1+n_2h_2+3n_3h_3)] \times \langle \exp[i\mathbf{k}\cdot\boldsymbol{\delta}_{n3}]\rangle . \quad (36)$$

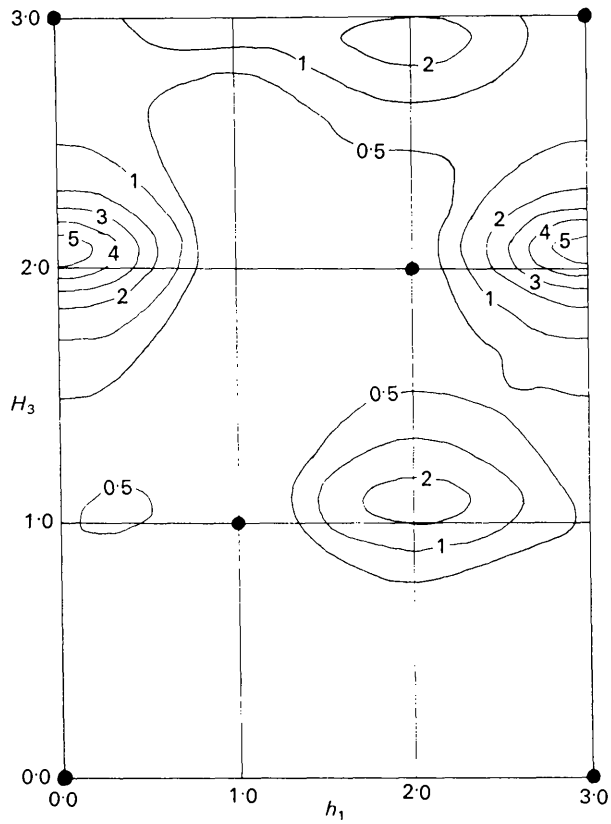

Fig. 3. The function $Q(h_1 0 H_3)$ for $u = \frac{1}{6}$.

Now, upon transformation, the atomic displacement is either $4c/9-c/3=a_3$ or $5c/9-2c/3=-a_3$. With κ_n and κ_0 defined as before, a parallel development follows leading to identical results, except that equation (24) becomes

$$Q(h_1h_2h_3)=\sum_{n_3}\psi_{n_3}\langle\exp[i\mathbf{k}\cdot\boldsymbol{\delta}_{n_3}]\rangle\exp[6\pi i n_3h_3]\,. \quad (37)$$

The meaning of ψ_{n_3} is unchanged.

Fig. 4 for $Q(h_10H_3)$ was computed from equation (37) with the same ψ_n's used for Fig. 3. Here $H_3=9h_3$

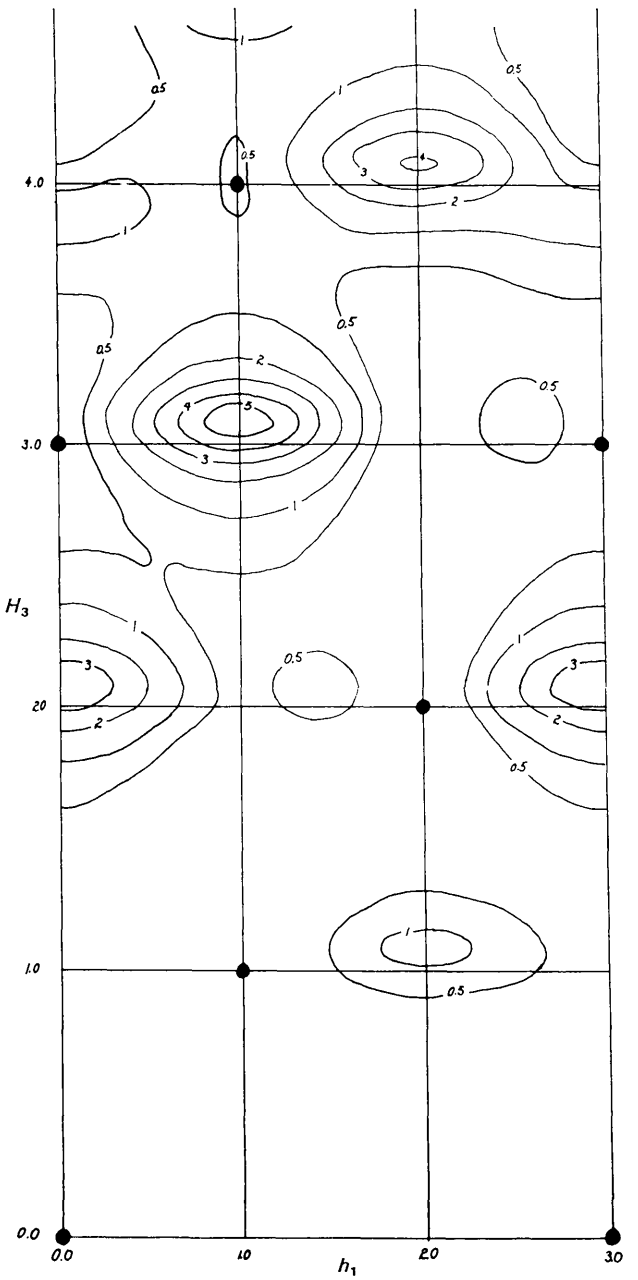

Fig. 4. The function $Q(h_10H_3)$ for $u=\frac{1}{9}$.

and the point $h_1, H_3=\frac{3}{2},\frac{9}{2}$ is an inversion center. The figure shows that we have successfully suppressed the 203 reflection while the intensity of $hkl=103$ remains strong, in qualitative agreement with observation.

The sense in which our calculation has failed is that though the diffuse superstructure maxima are shifted from the usual nodes of the reciprocal lattice parallel to **c***, all of the shifts shown in Figs. 3 and 4 are in the wrong direction. For example the 002 maximum is shown in the figures to be shifted away from the origin; it is invariably observed to be shifted inward.

We were convinced that this discrepancy must be related to the artificial state of order (a random distribution of the two equally likely structural entities in the vertical columns), or possibly the simple composition (one-quarter untransformed), or both. The theory was generalized in terms of a nearest-neighbor order parameter γ for the vertical columns, γ being the probability that an ω cell is followed by a β translational unit, and x, the fraction of the crystal untransformed. With the computer, the position of the 002 maximum was monitored for $0<\gamma<1$ and $0<x<1$. For no values of γ and x was the direction of the peak shift reversed. Hence no generalization of the model described here will agree with experiment.

This unexpected result forces us to conclude that we may not reproduce the intensity distribution using only the building blocks of the transformed and untransformed material. It is likely that there exist in the crystal local atomic configurations not found in either the β or ω phases.

At this time methods for the solution of short-range structure problems are sufficiently primitive that we may do little else than make reasonably plausible guesses. We have very little feel for how a particular local atomic configuration reflects itself in reciprocal space in terms of peak shift directions and the other quantitative properties of the intensity distribution.

In a companion paper the last in a series of models for the short-range structure of this alloy, which does reproduce quantitatively the experimentally observed intensity distribution, is described.

APPENDIX *A*

The probabilities P_p and $P_{p'}$

Consider a plane divided into an infinite number of small regions, T of which are distinctly different. We migrate in the plane, beginning in one of the regions. P_p is the probability that after having crossed p boundaries, we find ourselves in a region identical to the one containing the origin. P'_p is the probability that we are in a region different from that of the origin. We assume that on crossing a boundary it is equally likely that we enter any of the other $T-1$ different regions. Then

$$P_p+(T-1)P'_p=1\,. \quad (38)$$

Suppose that after having crossed $p-1$ boundaries, we find ourselves in a region different from that of the

origin. From such a region, the likelihood that the next boundary traversed will take us into an origin-like region is $1/(T-1)$. But there are $T-1$ origin-different regions for which such a result obtains. Hence

$$P_p=(T-1)P_{p-1}'/(T-1)=P_{p-1}'. \tag{39}$$

Combination of equations (38) and (39) to eliminate P_p' gives

$$P_p=(1-P_{p-1})/(T-1). \tag{40}$$

The general solution to a difference equation of this form is $P_p=a+bz^p$ where a, b, and z are constants. Its substitution into (40) gives

$$\{a-1/(T-1)+a/(T-1)\}+bz^{p-1}\{1/(T-1)+z\}=0.$$

Since this must be true for any p, we have $z=-1/(T-1)$ and $a=1/T$. So $P_p=1/T+b[-1/(T-1)]^p$. To find b we use the boundary condition that $P_0=1$, which gives $b=(T-1)/T$. So

$$P_p=1/T+[-1/(T-1)]^p(T-1)/T. \tag{41}$$

From equation (38),

$$P_p'=(1-P_p)/(T-1)=\{(T-1)/T-[-1/(T-1)]^p \times(T-1)/T\}/(T-1)=1/T-[-1/(T-1)]^p/T. \tag{42}$$

Equations (41) and (42) reduce to equations (8) and (9) of the text for the special case that $T=4$.

APPENDIX *B*

Properties of ψ_n

In order that the function $Q(h_1h_2h_3)$ be real, from equation (24) it is necessary that $\psi_n=\psi^*_{-n}$. Given that we have established the character of ω_1 and β regions (Fig. 2) by specifying configurations below the origin plane, it would appear that we have introduced a polarity into ψ_n; it is not obvious that ψ_n has this property. We prove that it does.

With $\sigma_{-n}=\sigma_n$ and with the convention established in Fig. 2, as before we compute the contribution to $\langle\exp[2\pi i(\kappa_{-n}-\kappa_0)h_3]\rangle$ for those atomic pairs which begin with the origin in an ω_2 subvariant:

$$\langle\exp[2\pi i(\kappa_{-n}-\kappa_0)h_3]\rangle_2=\tfrac{1}{4}\exp[2\pi ih_3]\{P_p(\sigma_{n_3-2}+\tfrac{1}{2}\sigma_{n_3-3}\exp[-2\pi ih_3]+\tfrac{1}{2}\sigma_{n_3-4}\exp[2\pi ih_3])+2P_p'(\sigma_{n_3-1}+\tfrac{1}{2}\sigma_{n_3-2}\exp[-2\pi ih_3]+\tfrac{1}{2}\sigma_{n_3-3}\times\exp[2\pi ih_3])+P_p'(\sigma_{n_3-3}+\tfrac{1}{2}\sigma_{n_3-4}\exp[-2\pi ih_3]+\tfrac{1}{2}\sigma_{n_3-5}\exp[2\pi ih_3])\}. \tag{43}$$

Equation (43) is the analog of equation (10) for n_3 negative. With P_p and P_p' eliminated with equations (8) and (9), and with $\mathscr{F}$ as defined by equation (13), we have

$$\langle\exp[2\pi i(\kappa_{-n}-\kappa_0)h_3]\rangle_2=\tfrac{1}{4}[1-(-\tfrac{1}{3})^p]\exp[2\pi ih_3]\mathscr{F}+\tfrac{1}{4}(-\tfrac{1}{3})^p(\sigma_{n_3-2}\exp[2\pi ih_3]+\tfrac{1}{2}\sigma_{n_3-3}+\tfrac{1}{2}\sigma_{n_3-4}\exp[4\pi ih_3]). \tag{44}$$

Similar expressions for the origin in ω_3, β, and ω_1 regions are

$$\langle\exp[2\pi i(\kappa_{-n}-\kappa_0)h_3]\rangle_3=\tfrac{1}{4}[1-(-\tfrac{1}{3})^p]\times\exp[-2\pi ih_3]\mathscr{F}+\tfrac{1}{4}(-\tfrac{1}{3})^p(\sigma_{n_3-1}\exp[-2\pi ih_3]+\tfrac{1}{2}\sigma_{n_3-2}\exp[-4\pi ih_3]+\tfrac{1}{2}\sigma_{n_3-3}); \tag{45}$$

$$\langle\exp[2\pi i(\kappa_{-n}-\kappa_0)h_3]\rangle_\beta=\tfrac{1}{4}[1-(-\tfrac{1}{3})^p]\mathscr{F}+\tfrac{1}{4}(-\tfrac{1}{3})^p(\sigma_{n_3-1}+\tfrac{1}{2}\sigma_{n_3-2}\exp[-2\pi ih_3]+\tfrac{1}{2}\sigma_{n_3-3}\exp[2\pi ih_3]); \tag{46}$$

$$\langle\exp[2\pi i(\kappa_{-n}-\kappa_0)h_3]\rangle_1=\tfrac{1}{4}[1-(-\tfrac{1}{3})^p]\mathscr{F}+\tfrac{1}{4}(-\tfrac{1}{3})^p(\sigma_{n_3-3}+\tfrac{1}{2}\sigma_{n_3-4}\exp[-2\pi ih_3]+\tfrac{1}{2}\sigma_{n_3-5}\exp[2\pi ih_3]). \tag{47}$$

Combination of equations (44), (45), (46), and (47) yields a result analogous to equation (19):

$$\langle\exp[2\pi i(\kappa_{-n}-\kappa_0)h_3]\rangle=\mathscr{F}^2+(-\tfrac{1}{3})^p\psi_{-n_3}$$

with

$$\psi_{-n_3}=(\tfrac{1}{2}\sigma_{n_3-3}+\tfrac{1}{4}\sigma_{n_3-1}-\tfrac{3}{8})+(\tfrac{1}{4}\sigma_{n_3-1}+\tfrac{1}{8}[\sigma_{n_3-2}\,\sigma_{n_3-4}]-\tfrac{1}{4})\exp[-2\pi ih_3]+(\tfrac{1}{4}\sigma_{n_3-2}+\tfrac{1}{8}[\sigma_{n_3-3}\,\sigma_{n_3-5}]-\tfrac{1}{4})\exp[2\pi ih_3]+(\tfrac{1}{8}\sigma_{n_3-2}-\tfrac{1}{16})\exp[-4\pi ih_3]+(\tfrac{1}{8}\sigma_{n_3-4}-\tfrac{1}{16})\exp[4\pi ih_3]. \tag{48}$$

To show that equation (48) is simply the complex conjugate of equation (18) an identity is required. Since the origin may with equal probability be followed by a β entity, which advances n_3 by one, or an ω cell, which advances it by three, it follows that

$$\sigma_n=\tfrac{1}{2}\sigma_{n-1}+\tfrac{1}{2}\sigma_{n-3}. \tag{49}$$

If we use equation (49) to eliminate σ_{n_3-1} in terms of σ_{n_3} and σ_{n_3-3} in the first parenthesis of equation (48), to eliminate $\sigma_{n_3-2}+\sigma_{n_3-4}$ in the second, and $\sigma_{n_3-3}+\sigma_{n_3-5}$ in the third, we have $\psi_{-n_3}=\psi^*_{n_3}$. Equation (49) might have been used as an alternative to (12) for a recursion formula for the generation of the σ_n's.

In writing equations (10) through (16) leading to equation (18) for ψ_{n_3}, we began in a particular kind of region, translated in the hexagonal plane $n_1\mathbf{a}_1+n_2\mathbf{a}_2$ crossing p boundaries, and then translated $n_3\mathbf{a}_3$ to account for the average relative phases for $n_1n_2n_3$ atomic pairs. However, our result for ψ_{n_3} must be independent of the path followed. We show that beginning in an ω_2 region, we may reverse the sequence of the two translations and still obtain equation (10). We have

$$\langle\exp[2\pi i(\kappa_n-\kappa_0)h_3]\rangle_2=\tfrac{1}{4}\exp[2\pi ih_3]\{\sigma_{n_3-1}(P_p+P_p'\{1+\exp[2\pi ih_3]+\exp[-2\pi ih_3]\})+\tfrac{1}{2}\sigma_{n_3-2}(P_p\exp[2\pi ih_3]+P_p'\{2+\exp[-2\pi ih_3]\})+\tfrac{1}{2}\sigma_{n_3-3}(P_p\exp[-2\pi ih_3]+P_p'\{2+\exp[2\pi ih_3]\})\}. \tag{50}$$

Here after beginning in ω_2, σ_{n_3-1} is the probability that a translation of $n_3\mathbf{a}_3$ terminates on an undisplaced plane, that is, in ω_1 or β. P_p is the probability that the

terminal atom in the pair is in an identical region after the hexagonal translation. The coefficient of P'_p, $1+\exp[2\pi i h_3]+\exp[-2\pi i h_3]$, accounts for the ways in which the terminal atom may be in regions different from that found for the $n_3\mathbf{a}_3$ translation. The coefficients of $\frac{1}{2}\sigma_{n_3-2}$, the probability that the $n_3\mathbf{a}_3$ translation terminates on an atom displaced upward, and $\frac{1}{2}\sigma_{n_3-3}$, that it be displaced downward, are similarly obtained.

After rearrangement equation (50) becomes

$$\langle \exp[2\pi i(\kappa_n-\kappa_0)h_3]\rangle_2 = \tfrac{1}{4}\exp[2\pi i h_3]\{P_p(\sigma_{n_3-1}+\tfrac{1}{2}\sigma_{n_3-2}\exp[2\pi i h_3]+\tfrac{1}{2}\sigma_{n_3-3}\exp[-2\pi i h_3]) + P'_p([\sigma_{n_3-1}+\sigma_{n_3-2}+\sigma_{n_3-3}]+[\sigma_{n_3-1}+\tfrac{1}{2}\sigma_{n_3-3}] \times \exp[2\pi i h_3]+[\sigma_{n_3-1}+\tfrac{1}{2}\sigma_{n_3-2}]\exp[-2\pi i h_3])\}. \quad (51)$$

With the aid of identity (49), equation (51) may be reduced to equation (10). Since equations (15) and (16) are similarly independent of the translational sequence, equation (18) for ψ_{n_3} must be as well.

APPENDIX C
The lattice sum $G(h_1h_2)$

Given the conventional choice of hexagonal axes, as indicated in Fig. 5, we must avoid counting translational combinations such as $\mathbf{a}_1+\mathbf{a}_2$ as two chances for a boundary, since the resultant vector is itself only a single translation. To avoid this ambiguity, we must compute the sum by sextants and combine them to obtain the final result.

With reference to Fig. 5, the lattice points in region I have coordinates $n_1\mathbf{a}_1+n_2(-\mathbf{a}_2)$, $\mathbf{n}_1$ and $\mathbf{n}_2$ being any non-negative integer. Then the contribution to G, defined schematically by equation (23), from region I is

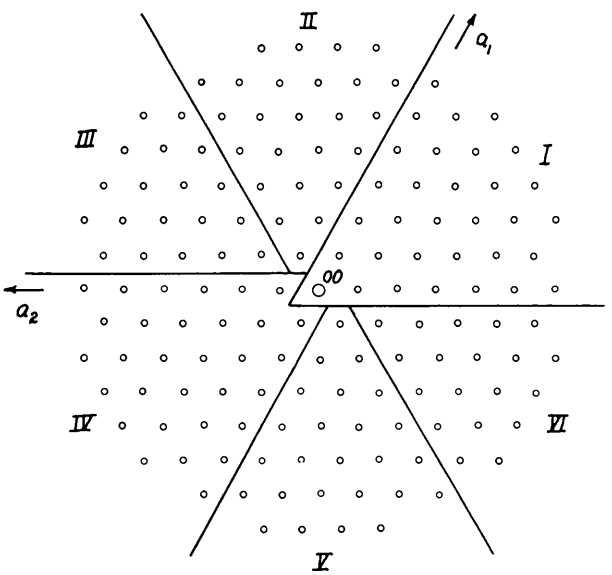

Fig. 5. Construction for the evaluation of $G(h_1h_2)$.

$$\sum_{n_1=0}^{\infty}(\eta\exp[2\pi i h_1])^{n_1}\sum_{n_2=0}^{\infty}(\eta\exp[-2\pi i h_2])^{n_2} = 1/(1-\eta\exp[2\pi i h_1])\,(1-\eta\exp[-2\pi i h_2]).$$

The contribution from region IV is simply the complex conjugate of this result minus one, since the origin is excluded from that region. The combination of these two sums after some simplification reduces to

$$\mathrm{I}+\mathrm{IV} = \frac{1-2\eta^2\cos 2\pi(h_1+h_2)+\eta^4}{(1-2\eta\cos 2\pi h_1+\eta^2)(1-2\eta\cos 2\pi h_2+\eta^2)} - \frac{\eta^2}{1-2\eta\cos 2\pi h_1+\eta^2} - \frac{\eta^2}{1-2\eta\cos 2\pi h_2+\eta^2}. \quad (52)$$

In region II, the lattice points may be specified by $n_1(\mathbf{a}_1+\mathbf{a}_2)+n_2\mathbf{a}_1$ with $1\le n_1$ and $0\le n_2$. Hence

$$\mathrm{II} = \sum_{n_1=1}^{\infty}(\eta\exp[2\pi i\{h_1+h_2\}])^{n_1}\sum_{n_2=0}^{\infty}(\eta\exp[2\pi i h_1])^{n_2} = \frac{\eta\exp[2\pi i\{h_1+h_2\}]}{(1-\eta\exp[2\pi i\{h_1+h_2\}])\,(1-\eta\exp[2\pi i h_1])}.$$

Combination of this result with its complex conjugate gives the contribution to G from regions II and V. After simplification there results

$$\mathrm{II}+\mathrm{V} = \frac{1-2\eta^2\cos 2\pi h_2+\eta^4}{(1-2\eta\cos 2\pi h_1+\eta^2)(1-2\eta\cos 2\pi\{h_1+h_2\}+\eta^2)} - \frac{1}{1-2\eta\cos 2\pi h_1+\eta^2} - \frac{\eta^2}{1-2\eta\cos 2\pi\{h_1+h_2\}+\eta^2}. \quad (53)$$

The lattice points are given by $n_1(\mathbf{a}_1+\mathbf{a}_2)+n_2\mathbf{a}_2$ in region III, and the lower bounds are $1\le n_1$ and $1\le n_2$. Thus

$$\mathrm{III} = \sum_{n_1=1}^{\infty}(\eta\exp[2\pi i\{h_1+h_2\}])^{n_1}\sum_{n_2=1}^{\infty}(\eta\exp[2\pi i h_2])^{n_2} = \frac{\eta^2\exp[2\pi i\{h_1+2h_2\}]}{(1-\eta\exp[2\pi i\{h_1+h_2\}])\,(1-\eta\exp[2\pi i h_2])}.$$

One finds that

$$\mathrm{III}+\mathrm{VI} = \frac{2\eta^2\cos 2\pi\{h_1+2h_2\}-2\eta^2}{(1-2\eta\cos 2\pi\{h_1+h_2\}+\eta^2)(1-2\eta\cos 2\pi h_2+\eta^2)} + \frac{\eta^2}{1-2\eta\cos 2\pi h_2+\eta^2} + \frac{\eta^2}{1-2\eta\cos 2\pi\{h_1+h_2\}+\eta^2}. \quad (54)$$

On combination of (52), (53), and (54) there obtains

$$G(h_1h_2) = \{1-3\eta^2-3\eta^4+\eta^6-2\eta^2(1-\eta)^2[\cos 2\pi h_1+\cos 2\pi h_2+\cos 2\pi(h_1+h_2)]+4\eta_3[\cos^2 2\pi h_1+\cos^2 2\pi h_2+\cos^2 2\pi(h_1+h_2)-2\cos 2\pi h_1\cos 2\pi h_2\times\cos 2\pi(h_1+h_2)]\}/\{[1-2\eta\cos 2\pi h_1+\eta^2][1-2\eta\times\cos 2\pi h_2+\eta^2][1-2\eta\cos 2\pi(h_1+h_2)+\eta^2]\}. \quad (55)$$

Equation (55) for G in closed form behaves as described in the text. It reduces to unity for $\eta=0$, and with increasingly large η it generates sharp maxima at integral h_1 and h_2.

References

BAGARYATSKII, A., NOSOVA, G. J. & TAGUNOVA, T. V. (1955). *Dokl. Akad. Nauk. SSSR*, **105**, 1225–1228.

KEATING, D. T., AXE, J. D. & MOSS, S. C. (1973). In preparation.

SASS, S. L. (1972). *J. Less. Common Metals*, **28**, 157–173.

SASS, S. L. & BORIE, B. (1972). *J. Appl. Cryst.* **5**, 236–238.

SILCOCK, J. M., DAVIES, M. H. & HARDY, H. K. (1955). *Symposium on the Mechanism of Phase Transformations in Metals*, pp. 93–104. London: Institute of Metals.

YAKEL, H. L. (1972). Private communication.

Acta Cryst. (1973). A**29**, 594

The Short-Range Structure of Ti and Zr B.C.C. Solid Solutions Containing the ω Phase. II. Solution of the Structure Determination*

BY BERNARD BORIE,† STEPHEN L. SASS & ALF ANDREASSEN‡

Department of Materials Science and Engineering, Cornell University, Ithaca, New York 14850, *U.S.A.*

(*Received* 14 *December* 1972; *accepted* 11 *April* 1973)

Our new techniques for computing intensity distributions from atomic arrangements with defects in periodicity were applied to a variety of models in an attempt to reproduce in detail the diffuse neutron-diffraction pattern of a Zr–20 wt.% Nb alloy quenched from 1273°K. The model which succeeds is described, and its kinematic intensity sum is derived. The resultant computed diffuse intensity distribution is compared with experiment.

Introduction

In a companion paper (Borie, Sass & Andreassen, 1973, referred to here as Part I), the calculation of diffuse intensity distributions in reciprocal space resulting from the formation of the ω phase in b.c.c. solid solutions was described. The theory correctly separates the diffraction pattern into two parts: sharp fundamental Bragg maxima (those common both to b.c.c. and ω); and superstructure reflections, the details of which depend on the model used to specify the atomic positions. For a simple model, broadened superstructure maxima, forming planes of diffuse intensity whose normal is **c*** (the hexagonal basis vector of the reciprocal unit cell of the ω phase) were found. Though this result is qualitatively compatible with experiment, the model failed to reproduce the details of the observed intensity distribution. Specifically, superstructure peak shifts parallel to **c*** were found which are opposite in direction to those observed. Though relative intensities of the superstructure maxima derived from the model agreed qualitatively with experiment, a quantitative fit was not attempted.

* Research sponsored by the U. S. Atomic Energy Commission under contract with the Union Carbide Corporation, the Metallurgy Branch of the U. S. Office of Naval Research, and the U. S. Air Force.

† Also at the Metals and Ceramics Division, Oak Ridge National Laboratory, Oak Ridge, Tennessee 37830, U.S.A.

‡ Present Address: The Applied Physics Laboratory of Johns Hopkins University, Howard County Facility, 8623 Georgia Avenue, Silver Spring, Maryland 20910.

The model tested in Part I was that of a crystal composed of regions of either untransformed b.c.c. (the β phase), or wholly transformed ω, containing no fragments of ω cells. Diffuse effects and peak shifts were taken to result from anomalous interference effects among the subvariants of the system, as illustrated in Fig. 1, Part I.

The result of our calculation displayed in Figs. 3 and 4 of Part I is valid only for the special composition $\frac{1}{4}\beta$, $\frac{3}{4}\omega$ (by volume), and for a random distribution of integral ω cells and β translational entities in columns parallel to **c***. Its generalization to arbitrary composition and states of order failed to reverse the peak shifts.

We conclude from this that the crystal probably contains local atomic configurations not found in either ω or β regions. If that be the case, the diffraction pattern provides few clues as to what such a configuration may be. At this point in our understanding of the solution of short-range structure problems, we are reduced to testing physically plausible models.

We describe here the last in a series of models, which reproduces quantitatively the observed diffraction pattern. The diffuse intensity distribution to be fit by theory was taken to be that of Keating, Axe & Moss (1973) shown in Fig. 1. Since it was measured with neutrons, it is relatively free of the double diffraction and dynamical effects which plague electron-diffraction patterns, and it is free of form factor effects which cause X-ray measurements to be of uneven statistical quality.

The contour map of Fig. 1 is the intensity distribution in the plane $k=0$ at 300°K for a Zr–20 wt.% Nb